ACS OMEGA

Article

http://pubs.acs.org/journal/acsodf

Graphene Plasmon Cavities Made with Silicon Carbide

Ke Li,[†,‡,∥] Jamie M. Fitzgerald,[‡,∥] Xiaofei Xiao,[*,‡,∥] Joshua D. Caldwell,[§] Cheng Zhang,[†] Stefan A. Maier,[‡] Xiaofeng Li,[*,†] and Vincenzo Giannini[‡,⊥]

[†]College of Physics, Optoelectronics and Energy, Collaborative Innovation Center of Suzhou Nano Science and Technology, Key Laboratory of Modern Optical Technologies of Education Ministry of China, Soochow University, Suzhou 215006, China

[‡]The Blackett Laboratory, Imperial College London, London SW7 2AZ, U.K.

[§]US Naval Research Laboratory, 4555 Overlook Avenue SW, Washington, D.C. 20375, United States

[⊥]Instituto de Estructura de la Materia (IEM-CSIC), Consejo Superior de Investigaciones Científicas, Serrano 121, 28006 Madrid, Spain

ABSTRACT: We propose a simple way to create tunable plasmonic cavities in the infrared (IR) range using graphene films suspended upon a silicon carbide (SiC) grating and present a numerical investigation, using the finite element method, on the absorption properties and field distributions of such resonant structures. We find at certain frequencies within the SiC reststrahlen band that the structured SiC substrate acts as a perfect reflector, providing a cavity effect by establishing graphene plasmon standing waves. We also provide clear evidence of strong coupling phenomena between the localized surface phonon polariton resonances in the SiC grating with the graphene surface plasmon cavity modes, which is revealed by a Rabi splitting in the absorption spectrum. This paves the way to build simple plasmonic structures, using well-known materials and experimental techniques, that can be used to excite graphene plasmons efficiently, even at normal incidence, as well as explore cavity quantum electrodynamics and potential applications in IR spectroscopy.

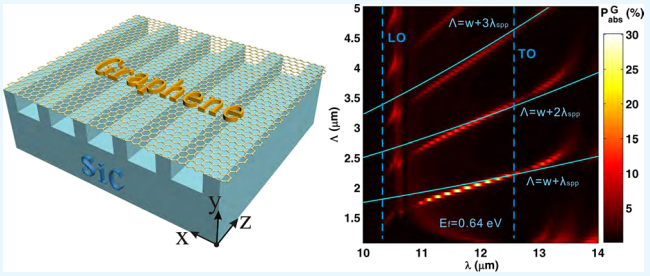

1. INTRODUCTION

Graphene is a two-dimensional (2D) single-atom thick layer of carbon, and after the experimental proof of existence in 2004,[1] its remarkable physical properties have led to one of the most prolific areas of research in nanoscience. In particular, its extreme 2D geometry and distinct band structure lead to novel interaction with light and have resulted in immense interest from the plasmonics and nano-optics communities.[2] Doped graphene supports collective oscillations of the free carriers known as surface plasmon polaritons (SPPs) that can be either propagating or localized[2,3] and has been recognized as a suitable alternative to noble metals in the field of plasmonics. These plasmonic modes are characterized by large field confinement [plasmon wavelengths, a 100 times smaller than the free-space wavelength, have been demonstrated at mid-infrared (IR) frequencies[4]] and enhancements and are particularly appealing in graphene because of the tunability of the Fermi energy via chemical doping or electrical gating. Optical gaps of up to 2 eV (which corresponds to $E_F \approx 1$ eV) can be created.[5] This paves the way for cheap, reliable, and ultrafast optical modulators. At terahertz and IR frequencies, graphene plasmons have been conclusively demonstrated by a number of different experimental techniques including scanning near-field microscopy,[6−8] optical far-field spectroscopy,[9] and electron energy loss spectroscopy.[10]

Silicon carbide (SiC) is a polar dielectric that supports subdiffraction confinement of light using the excitation of surface phonon polaritons (SPhPs) that result from the coupling of a photon with the collective oscillation of the polar lattice atoms.[11] Because of the energy scale of optical phonons, the reststrahlen band [a narrow and material-dependent frequency range bounded by the longitudinal optical (LO) and transverse optical (TO) phonon frequencies] inherently occurs within the IR to terahertz regime, where polar dielectrics act as an optical metal, that is, they exhibit high reflectivity and negative real part of the dielectric function. The long phonon lifetimes (picoseconds), as compared to electron scattering times in metals (10s of femtoseconds), means that the imaginary part of the dielectric function can be orders of magnitude smaller than that for noble metals, leading to low-loss systems with high quality factors and narrow line widths.[11] As previously shown, nanostructuring SiC results in localized surface phonon polaritons (LSPhPs) with a high Q and strong field confinement.[12,13] SiC also has a large band gap and high thermal, mechanical, and chemical stability, making it highly suitable for a number of applications.

In this work, we explore the coupling between SiC LSPhPs and graphene SPPs and explore the unique properties of the hybrid modes,[14] which combine positive characteristics of the graphene SPPs (large light confinement and tunable) and SiC

Received: June 4, 2017
Accepted: June 20, 2017
Published: July 14, 2017

DOI: 10.1021/acsomega.7b00726
ACS Omega 2017, 2, 3640−3646

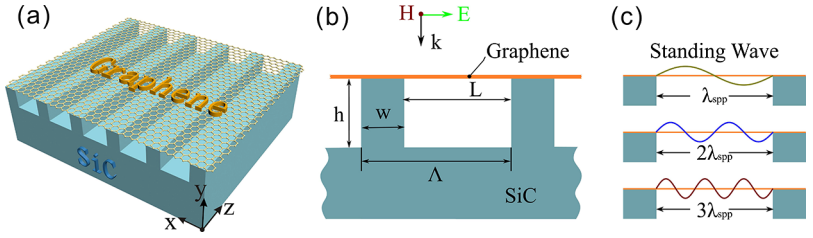

Figure 1. Schematics of the SiC grating and graphene plasmonic device. (a) Three-dimensional view of the whole structure and (b) cross-sectional view (the incident light is transverse magnetic (TM) polarized normal incident in the air, where Λ is the grating period, *w* is the width of the grating ridge, *L* is the width of the grating groove, and *h* is the grating height). (c) Sketch of the standing waves of graphene SPP resonance in a grating cavity.

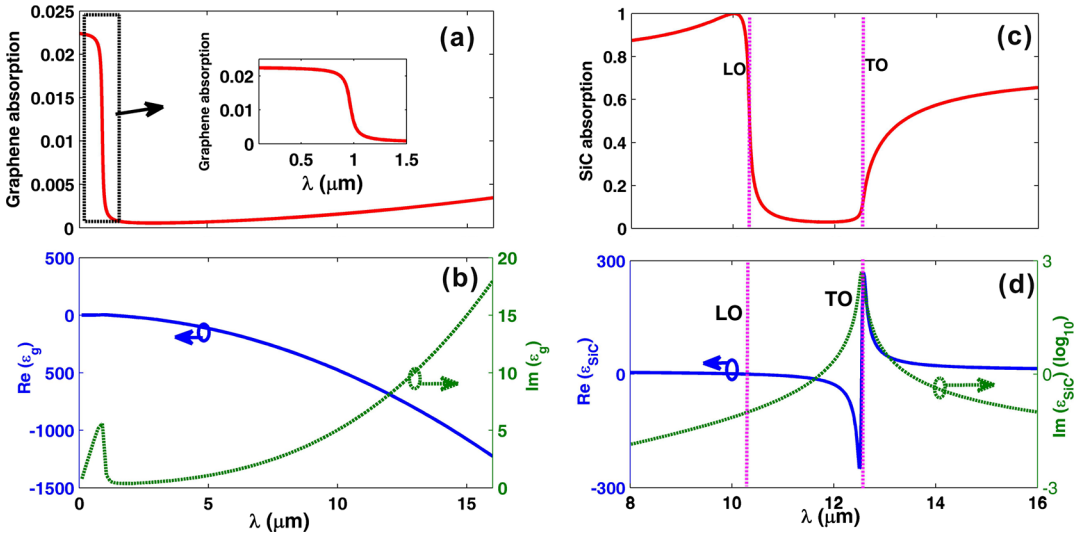

Figure 2. Material properties of single-layer graphene in air (a,b) and bulk SiC (c,d). The chemical potential of graphene is E_F = 0.64 eV, and carrier mobility is μ = 10 000 cm^2/(V s) in all our simulations unless otherwise specified. (a) Absorption of graphene: from the inset, it is shown that graphene has remarkably high absorption at visible light range. (b) Permittivity of graphene. (c) SiC absorption and its reststrahlen band. (d) Permittivity of SiC.

LSPhPs (low loss). We consider a single-layer graphene sheet on the top of a SiC cavity. Structuring of SiC[12,13] leads to the excitation of both the graphene SPP and a LSPhP in SiC. This is convenient as the difficulty in nanofabrication of graphene devices, as well as the large momentum mismatch between graphene SPPs and the incident light, means that the creation of graphene-based resonators that can be excited at normal incidence, is challenging. A numerical investigation, using finite element analysis method from COMSOL Multiphysics, on the absorption properties and field distributions of this system in the IR range is reported. At frequencies in the reststrahlen band, but away from the LSPhP resonances, SiC acts as a "perfect conductor", and at certain lengths of the grating groove, a plasmon standing wave is set up. Here, by a perfect conductor, we simply mean that the real part of the permittivity is extremely large and negative (small field penetration), and we assume that SiC is undoped and hence is not conductive. This setup is a different way to excite localized graphene plasmons and achieve strong resonant absorption, without using nanoribbons. Note that although we consider the cavity as part of a periodic structure (i.e., a grating that is convenient for experiments and numerical simulations), we do not consider the excitation of modes using diffraction. The necessary momentum is provided by the abrupt breaking of the symmetry of the cavity, not by the periodicity.[a]

There is a lot of interest on the coupling of surface phonons and graphene plasmons, which becomes important at the mid-IR range for typical polar dielectric substrates such as SiC[15,16] and SiO_2.[6,17,18] It has also been demonstrated in graphene/hexagonal boron nitride (h-BN) heterostructures[4,19−22] and thin layers of surface-absorbed polymers.[23] Recently, the interaction of localized plasmons in a gold antenna with a SiO_2 coating and the substrate has been explored, and it was found that strong coupling between the modes leads to a transparency window.[24] We find, near the LO phonon frequency, a strong interaction between the LSPhPs and the graphene plasmons, leading to Rabi splitting, signaling the coherent energy transfer between the two coupled modes.[25,26] The high quality factor *Q* and the small effective volume *V* of the hybrid modes make this system a suitable system for cavity quantum electrodynamics (QED)[27] where one is interested in the strong mixing of light and individual emitters. In photonic cavities, the modal volume is on the order of λ^3, but by using localized surface plasmons (LSPs) and/or LSPhPs, one can confine light fields evanescently and achieve subdiffraction modal volume. Using hybrid modes to tailor the spectral and spatial profile of localized plasmons to aid strong coupling to emitters has been demonstrated.[28] By picking suitable constituent modes that have complimentary characteristics, the *Q*/*V* ratio, which is proportional to the Purcell factor, can be increased to enhance strong light−matter interactions with

DOI: 10.1021/acsomega.7b00726
ACS Omega 2017, 2, 3640−3646

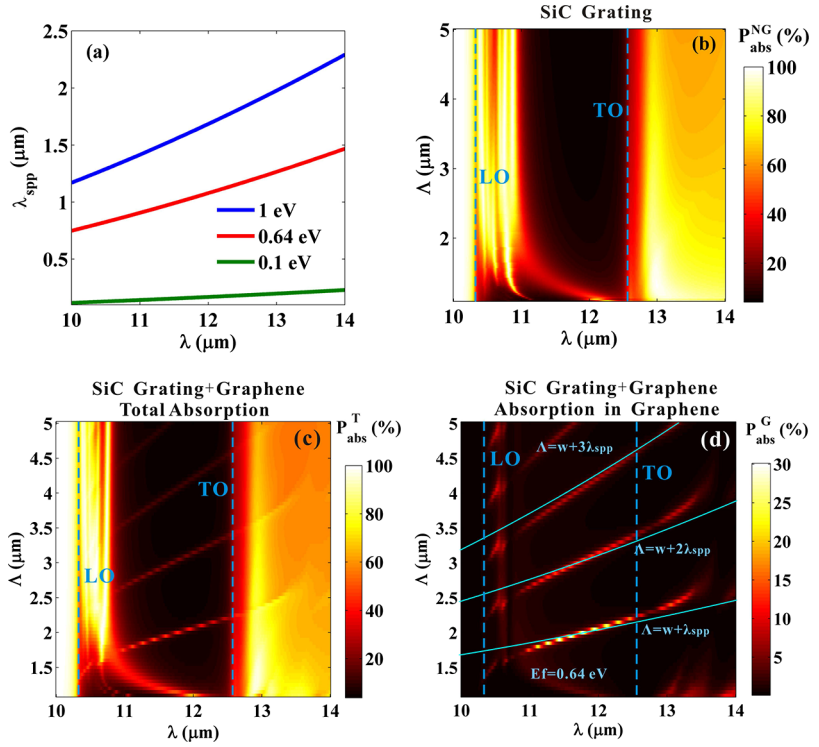

Figure 3. (a) Graphene SPP wavelength for different values of the chemical potential. (b) Total absorption (P_{abs}^{NG}) vs grating period (Λ) and incident wavelength (λ) for the SiC grating (with no graphene) structure for $w = h = 1$ μm. (c) Total absorption (P_{abs}^{T}) vs grating period and incident wavelength for the SiC grating and graphene structure for $w = h = 1$ μm. (d) Absorption of the graphene layer (P_{abs}^{G}) vs grating period and incident wavelength for the SiC grating and graphene structure for $w = h = 1$ μm. The blue lines indicate a fit to a Fabry–Pérot model for a phase shift of $-\pi$ (see eq 4).

emitters. Our work provides a potential method to efficiently excite unique hybrid modes for confining and manipulating light and could pave the way for applications in tunable broadband molecular spectroscopy in the terahertz and IR range.[29] Furthermore, the device potentially provides a new system to study cavity QED. The high quality factor and the small modal volume make this system a very suitable platform for inducing and exploring strong light–matter interactions.

2. RESULTS AND DISCUSSION

In Figure 1, we show the system to be studied. It is composed of a monolayer graphene sheet deposited on a SiC grating, and we assume that the two are in physical contact with one another. The graphene sheet is located on the x–z plane with the grating period in the x direction. The incident light propagates in the y direction from above and is normal to the graphene surface. It is TM so that SPPs can be excited above the grating in the graphene layer. The height, period, ridge width, and groove width of the grating are, respectively, represented by the letters h, Λ, w, and L (see Figure 1b). The graphene thickness in the simulations is 0.5 nm, which we have checked is converged for all results. The cavity supporting the graphene SPPs is given by the zone where the graphene is suspended (see Figure 1c).

We model the optical properties of graphene using the local random phase approximation model that is known to work well.[2,30] We also use the zero-temperature limit that is a good approximation even for finite temperatures. The conductivity is given by

$$\sigma(\omega) = \frac{e^2 E_F}{\pi\hbar^2}\frac{i}{\omega + iT^{-1}} + \frac{e^2}{4\hbar^2}\left(\theta(\hbar\omega - 2E_F) + \frac{i}{\pi}\log\left(\left|\frac{\hbar\omega - 2E_F}{\hbar\omega + 2E_F}\right|\right)\right) \quad (1)$$

where τ is the carrier relaxation time and is linked to the carrier mobility μ via the equation $\tau = \frac{\mu E_F}{e v_F^2}$, θ denotes a step function, and E_F is the Fermi energy. The first term describes intraband transitions and is Drude-like. This will dominate the response over the second term, which describes interband transitions, at the frequencies and levels of doping we consider. In Figure 2a,b, we plot the corresponding dielectric function for $E_F = 0.64$ eV and $\mu = 10\,000$ cm^2/(V s) (which is a typical maximum value for the mobility of chemical-vapor-deposition-grown graphene), where it can be seen that graphene, for a single-layer structure, has a remarkably large absorption at visible wavelengths.

The dielectric function for polar dielectrics such as SiC can be described by a Lorentz oscillator model

$$\epsilon(\omega) = \epsilon_\infty\left(1 + \frac{\omega_{LO}^2 - \omega_{TO}^2}{\omega_{TO}^2 - \omega^2 - i\omega\gamma}\right) \quad (2)$$

which has a pole at the TO phonon frequency ω_{TO} and a zero-crossing point at θ_{LO}. For SiC,[31] $\epsilon_\infty = 6.56$, $\omega_{LO} = 973$ cm^{-1}, $\omega_{TO} = 797$ cm^{-1}, and $\gamma = 4.76$ cm^{-1}; in Figure 2c,d, we show the absorption and permittivity of SiC. The SPhPs can only be supported in a narrow spectral bandwidth (in the case of SiC around 176 cm^{-1}), but crucially they correspond to frequencies

DOI: 10.1021/acsomega.7b00726
ACS Omega 2017, 2, 3640–3646

at which graphene plasmons can be excited, paving the way for interactions between the two types of excitations.

If the momentum mismatch is overcome, graphene SPPs can be excited by the normal incident light. Assuming that interband transitions can be ignored, the dispersion relation for the plasmon waves in a free-standing graphene sheet is given by[30]

$$k_{\mathrm{SPP}}(\omega) = \frac{\pi\hbar^2\epsilon_0(\epsilon_1+\epsilon_2)}{e^2E_{\mathrm{F}}}\left(1+\frac{\mathrm{i}}{\omega\tau}\right)\omega^2 \quad (3)$$

where k_{SPP} is the in-plane wavevector of the plasmon and ϵ_1 and ϵ_2 are the relative permittivity of the materials in the infinite half-spaces above and below the graphene sheet, respectively. The dispersion is plotted in Figure 3a for a graphene sheet in vacuum for different levels of doping; the dispersion curve indicates that the plasmon wavelength is on the order of 10−100 times smaller than the incident wavelength, revealing the large confinement and the consequent momentum mismatch that must be overcome for efficient coupling. Unless otherwise specified, we use a Fermi energy of 0.64 eV throughout this work.

To investigate our system, we begin by calculating the absorption of a SiC grating with no graphene sheet present. We assume that SiC is infinitely thick below the grating to switch off the transmission channel and simplify the analysis. We consider wavelengths and grating periods in the range 10−14 and 1.1−5 μm, respectively, with the grating height and the ridge width fixed at 1 μm. The results are shown in Figure 3b. We see that within the reststrahlen band there is now a number of peaks as compared to the plain SiC case (Figure 2c); this is due to the interaction of the LO phonon and the grating, which leads to the excitation of LSPhPs.[13] There is a region of large absorption at the LSPhP resonances, but elsewhere in the band the absorption is close to 0% as SiC acts as a perfect reflector. Outside of the reststrahlen band, for frequencies less than ω_{LO} and larger than ω_{TO}, the absorption is very similar to that for a plain SiC surface shown in Figure 2c.

Next, we add graphene on the top of the grating, with the results shown in Figure 3c,d. We consider two quantities: $P^{\mathrm{T}}_{\mathrm{abs}}$, which represents the total absorption (sum of the absorption of the SiC grating and the graphene layer), and $P^{\mathrm{G}}_{\mathrm{abs}}$, which is the absorption in the graphene. The most striking difference is the appearance of strong absorption peaks in the low absorption region of the reststrahlen band for certain grating period lengths. This can be understood by looking at the near field of the y component of the electric field for each peak, as shown in Figure 4a. The field is concentrated in the graphene layer and has a fixed number of wavelengths in the region directly over air. The plasmon modes are antisymmetric, which is a consequence of the electric field boundary conditions. The normal incident field excites SPPs at the edge, which are out of phase and will only constructively interfere for odd modes.[32] In the parts of the graphene, which are located on the top of SiC, there exists a very weak field and consequently there is low absorption in these locations. This can be understood by noting in this spectral region that SiC acts, to a good approximation, as a perfect electrical conductor and screens out any external field very effectively. In other words, the field is zero outside of the cavity region and leads to plasmon standing waves being established. To confirm this, in Figure 4a, we show the absorption varying with the cavity length (for a fixed wavelength λ = 12 μm). We find, at integer multiples of L/λ_{SPP}, absorption peaks that correspond to the plasmon standing waves. This is shown pictorially in Figure 1c. For non-normal incident light, it is also possible to excite symmetric plasmon standing waves as the symmetry of the system is broken. Note that there is also a small peak located near L/λ_{SPP} = 0, which is a LSPhP mode that is visible without graphene (see Figure 3b); it is present for small cavities because of near-field coupling between the two SiC slabs. Our findings have some similarities with earlier work on the plasmonic coupling between graphene SPPs and magnetic polaritons in silver gratings.[33] Note that the cavities used in that work are very deep (a width of 300 nm and a height of 2 μm) as compared to that of our system, where the cavity height and the width studied are always equal or comparable, which makes the experimental realization potentially much simpler. The highest field enhancement in our system is located on the graphene layer, which is very convenient for potential applications in molecular sensors. Note that the fact that the peak position does not change for varying Λ (for a fixed cavity length) is a confirmation that these are localized cavity modes and are not modes excited by diffraction effects owing to the grating periodicity.[34] In an experiment, it would be more natural to explore these standing wave modes by scanning the excitation light wavelength for fixed geometric parameters; in Figure 4b, we show this for various chemical potentials for L = 1.06 μm, w = 2.0 μm, and h = 1 μm. We find that as the Fermi energy is increased the absorption peak red shifts (as the SPP wavelength changes with E_{F}) and grows in intensity. This illustrates that our system can act as a tunable cavity, thanks to the inclusion of the graphene sheet. In Figure 4c, we show how the grating height impacts the absorption of graphene; we find that the absorption intensity is

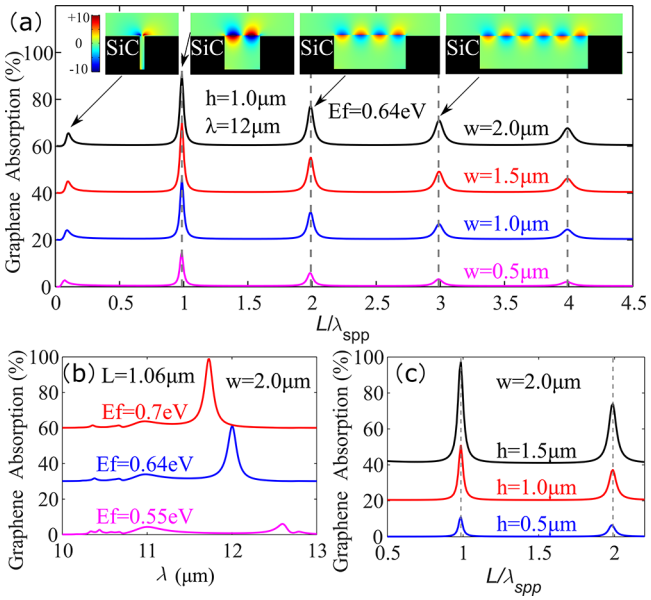

Figure 4. (a) Absorption of the graphene layer at different geometric parameters L/λ_{SPP} of the SiC grating. The peaks at integer numbers of L/λ_{SPP} correspond to the standing waves of the graphene SPPs as indicated by the above near-field plot of E_y for each peak. The electric field (here, normalized to the incident field magnitude) goes to zero at the boundaries, meaning that the plasmon modes must be antisymmetric. (b) Absorption of the graphene layer against excitation wavelength for fixed geometric parameters: L = 1.06 μm, w = 2.0 μm, and h = 1 μm (shown for different Fermi energies). (c) Absorption of the graphene layer at different geometric parameters for different grating heights h and E_{F} = 0.64 eV.

DOI: 10.1021/acsomega.7b00726
ACS Omega 2017, 2, 3640−3646

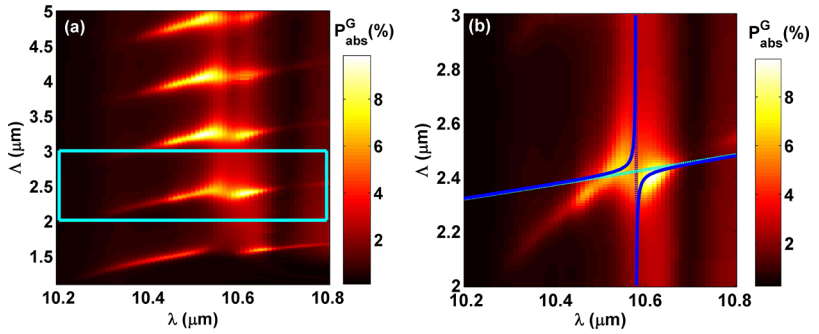

Figure 5. (a) Zoom-in of the absorption in the graphene layers (for $w = h = 1$ μm) shown in Figure 3d between the wavelengths 10.2 and 10.8 μm, highlighting the Rabi splitting for different modes. (b) Zoom-in for $m = 2$ mode (the purple dashed line indicates the LSPhP wavelength and the cyan dashed line shows the graphene SPP dispersion using the Fabry–Pérot model with a phase shift of -1.35π). The blue line shows the resulting splitting of the hybrid mode.

strongly dependent on the height. When the height is changed, the graphene SPP wavelength does not change; this is because when h is large (h > 500 nm here), then eq 3 applies and λ_{SPP} depends only on the material directly above and below the suspended graphene (in this case, air).

To confirm our intuition about these standing wave modes, we use the graphene dispersion in eq 3 along with a Fabry–Pérot model

$$\delta\phi + \Re(k_{SPP}(\omega))L = m\pi \tag{4}$$

where $\delta\phi$ is the phase shift. Taking a phase shift of $-\pi$, we find a good agreement with the simulation results (see the blue lines in Figure 3d) in the region near the TO energy where the grating acts as a perfect electric conductor (i.e., plasmon standing waves in the cavity). At frequencies away from this, the simple model breaks down as the phase shift is frequency-dependent and will differ from $-\pi$. This is due to the grating not acting as a perfect reflector any more and allowing some field penetration into the SiC. To quantify the suitability of the cavity as an experimental system for strong light–matter interactions, we consider the ratio Q/V. To calculate the volume, we consider a square cavity (with sides of length L, we use $w = 1$ μm and L is calculated using a period Λ that sets up a plasmon standing wave) with a plasmon standing wave setup in both directions; the dimension perpendicular to the graphene sheet is given by the out-of-plane decay of the plasmon: $\sim 1/\Re[k_{SPP}(\omega)][k_{SPP}(\omega)]$[35] (as $k_{SPP} \gg 2\pi/\lambda$, then $k_z \approx ik_{SPP}$, and for 12 μm incident wavelength, this distance corresponds to 0.17 μm). The quality factor can be estimated using the equation $Q \approx \omega/\Delta\omega$, where we obtain the line width $\Delta\omega$ using a Lorentzian fit. At a wavelength of 12 μm, we find a value of $Q/V = 8 \times 10^5/\lambda_0^3$, which is comparable to the values found for other graphene nanoresonators.[4]

Another interesting feature, revealed in Figure 3d (and a zoom-in is provided in Figure 5a,b), is the presence of an anticrossing point in the absorption spectrum close to the LO phonon frequency; this is a manifestation of strong coupling between the two modes, the graphene plasmon and a localized cavity SPhP,[13] and can be intuitively understood by considering two coupled harmonic oscillators.[26] The shape of the Rabi splitting shown in Figure 5a,b is a consequence of the dispersive graphene SPP (given by eq 4) and the LSPhP at a fixed wavelength of 10.6 μm. The strong coupling regime is very dependent on the level of the damping of the system; thus, the small line widths of graphene plasmons and SiC SPhPs are favorable for the observation of Rabi splitting. It should be noted that at frequencies close to the LO phonon energy graphene SPPs can become lossy because of substrate phonons.[4] In our cavity-grating system, a substantial amount of the graphene is free-standing and not in contact with the substrate, which should negate this.

In Figure 6, we show a slice of the absorption in the graphene, apply a sum of two Lorentzian functions to fit the

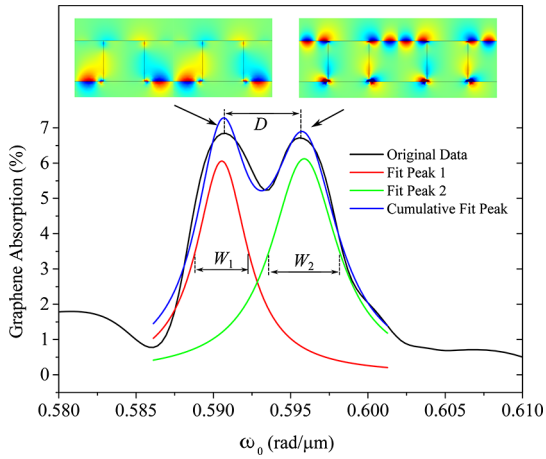

Figure 6. Spectra shown correspond to $L = 1.45$ μm, which means that $\Lambda = 2.45$ μm. The summation of two Lorentz equations is used to fit these peaks. The full widths at half maximum of these two peaks are 0.004 rad/μm (W_1) and 0.005 rad/μm (W_2). The peak distance is D = 0.005 rad/μm. The ratio $D/W = 1$ quantifies the strength of the coupling and shows that this is the strong coupling regime.

curve, and quantify the strength of the coupling. We find the peak separation (i.e., the Rabi splitting) to be $\omega_R = 1$ meV. This value can then be used with a coupled harmonic oscillator model to describe the anticrossing[36]

$$E_{\pm}(\omega) = \frac{\hbar\omega_{SPP} + \hbar\omega_{SPhP}}{2} \pm \frac{1}{2}\sqrt{(\hbar\omega_R)^2 + (\hbar\omega_{SPP} - \hbar\omega_{SPhP})^2} \tag{5}$$

where we take the LSPhP energy to be fixed at a value of 0.12 eV, the graphene SPP dispersion is given by eqs 3 and 4, and we use the phase shift as a fitting parameter as it can no longer be expected to be $-\pi$ at these wavelengths. The result for the fit to the $m = 2$ mode is shown in Figure 5b, where a good fit is

DOI: 10.1021/acsomega.7b00726
ACS Omega 2017, 2, 3640–3646

obtained using a phase shift of $\delta\phi = -1.35\pi$; this indicates that at these frequencies SiC does not act as a perfect reflector.

Also shown in Figure 6 are two near-field plots showing the different nature of the hybrid mode depending on the frequency; at lower frequencies, the mode is more phonon-polariton-like and the absorption is situated at the bottom of the cavity. At larger frequencies, the mode is more graphene-plasmon-like and the absorption is concentrated in the graphene layer on the top. Thus, over small frequency range, one has a lot of spatial control of where absorption takes place in this system, which is a consequence of strong coupling between the modes. Further control of the relative contribution of each mode is given by the cavity width and the doping level. To quantify the coupling, we compare the line width of the constituent modes (W_1 and W_2) to the splitting (D), for Rabi splitting to be experimentally observable $D \gtrsim W$.[26] Taking the largest line width, we get the ratio of $D/W = 1$, which justifies considering this interaction of the two modes as strong coupling.

3. CONCLUSIONS

We have studied a graphene and SiC cavity system and have shown its suitability as an experimentally realizable, tunable cavity that could be useful for cavity QED and molecular sensing in the mid-IR range. We have shown that the inclusion of a graphene monolayer on a SiC grating leads to a number of new modes in the low absorption part of the reststrahlen band. These modes can be explained as antisymmetric plasmon standing waves, set up by the SiC grating that acts as a perfect conductor at certain frequencies, which are well-explained by a simple Fabry–Pérot model. By altering the chemical potential of the graphene or changing the cavity width, one can change the spectral position of these peaks, meaning the system acts as a very tunable plasmonic cavity. Near the LO phonon energy, we find evidence of strong coupling between the graphene SPP and the LSPhP, leading to a hybrid mode[14] that exhibits characteristics of both constituent modes. Our results also offer promise that a similar coupling with local trace level quantities of molecules could be possible. We find that over a small frequency range the spatial profile of the hybrid modes can change significantly. The tunability, high quality factor, and low modal volume make this system an ideal setup for molecular sensing and to study cavity QED.

AUTHOR INFORMATION

Corresponding Authors

*E-mail: xx2215@ic.ac.uk (X.X.).
*E-mail: xfli@suda.edu.cn (X.L.).

ORCID

Jamie M. Fitzgerald: 0000-0003-3652-0676
Xiaofeng Li: 0000-0002-4115-3287

Author Contributions

‖K.L., J.M.F., and X.X. contributed equally to this work.

Author Contributions

All authors have given approval to the final version of the manuscript.

Notes

The authors declare no competing financial interest.

ACKNOWLEDGMENTS

K.L. was supported by China Postdoctoral Science Foundation (no. 2014M560444), Collaborative Academic Training Program for Postdoctoral Fellows of Collaborative Innovation Center of Suzhou Nano Science and Technology. The work of J.M.F. was supported under a studentship from the Imperial College London funded by the EPSRC grant 1580548. X.X. was supported by Lee Family Scholarship. S.A.M. acknowledges the Lee-Lucas Chair in Physics and the EPSRC Mathematical Fundamentals of Metamaterials Programme grant (EP/L024926/1), and V.G. acknowledges ONR Global funding (N62909-15-1-N082).

ADDITIONAL NOTE

[a]Proof of this is that the modes we explore are not reproduced by the equation $k_{SPP} = N\frac{2\pi}{\Lambda}$, where N is the diffraction order and Λ is the grating period. We consider a grating because it simplifies the calculation, but similar results would be obtained by a single cavity.

REFERENCES

(1) Novoselov, K. S.; Geim, A. K.; Morozov, S. V.; Jiang, D.; Zhang, Y.; Dubonos, S. V.; Grigorieva, I. V.; Firsov, A. A. Electric field effect in atomically thin carbon films. *Science* **2004**, *306*, 666–669.

(2) de Abajo, F. J. G. Graphene plasmonics: challenges and opportunities. *ACS Photonics* **2014**, *1*, 135–152.

(3) Maier, S. A. *Plasmonics: Fundamentals and Applications*; Springer Science & Business Media, 2007.

(4) Brar, V. W.; Jang, M. S.; Sherrott, M.; Lopez, J. J.; Atwater, H. A. Highly confined tunable mid-infrared plasmonics in graphene nanoresonators. *Nano Lett.* **2013**, *13*, 2541–2547.

(5) Chen, C.-F.; Park, C.-H.; Boudouris, B. W.; Horng, J.; Geng, B.; Girit, C.; Zettl, A.; Crommie, M. F.; Segalman, R. A.; Louie, S. G.; Wang, F. Controlling inelastic light scattering quantum pathways in graphene. *Nature* **2011**, *471*, 617–620.

(6) Fei, Z.; et al. Infrared nanoscopy of Dirac plasmons at the graphene–SiO_2 interface. *Nano Lett.* **2011**, *11*, 4701–4705.

(7) Fei, Z.; Rodin, A. S.; Andreev, G. O.; Bao, W.; McLeod, A. S.; Wagner, M.; Zhang, L. M.; Zhao, Z.; Thiemens, M.; Dominguez, G.; Fogler, M. M.; Neto, A. H. C.; Lau, C. N.; Keilmann, F.; Basov, D. N. Gate-tuning of graphene plasmons revealed by infrared nano-imaging. *Nature* **2012**, *487*, 82–85.

(8) Chen, J.; Badioli, M.; Alonso-González, P.; Thongrattanasiri, S.; Huth, F.; Osmond, J.; Spasenović, M.; Centeno, A.; Pesquera, A.; Godignon, P.; Elorza, A. Z.; Camara, N.; de Abajo, F. J. G.; Hillenbrand, R.; Koppens, F. H. L. Optical nano-imaging of gate-tunable graphene plasmons. *Nature* **2012**, *487*, 77–81.

(9) Ju, L.; Geng, B.; Horng, J.; Girit, C.; Martin, M.; Hao, Z.; Bechtel, H. A.; Liang, X.; Zettl, A.; Shen, Y. R.; Wang, F. Graphene plasmonics for tunable terahertz metamaterials. *Nat. Nanotechnol.* **2011**, *6*, 630–634.

(10) Shin, S. Y.; Kim, N. D.; Kim, J. G.; Kim, K. S.; Noh, D. Y.; Kim, K. S.; Chung, J. W. Control of the π plasmon in a single layer graphene by charge doping. *Appl. Phys. Lett.* **2011**, *99*, 082110.

(11) Caldwell, J. D.; Lindsay, L.; Giannini, V.; Vurgaftman, I.; Reinecke, T. L.; Maier, S. A.; Glembocki, O. J. Low-loss, infrared and terahertz nanophotonics using surface phonon polaritons. *Nanophotonics* **2015**, *4*, 44–68.

(12) Caldwell, J. D.; Glembocki, O. J.; Francescato, Y.; Sharac, N.; Giannini, V.; Bezares, F. J.; Long, J. P.; Owrutsky, J. C.; Vurgaftman, I.; Tischler, J. G.; Wheeler, V. D.; Bassim, N. D.; Shirey, L. M.; Kasica, R.; Maier, S. A. Low-loss, extreme subdiffraction photon confinement via silicon carbide localized surface phonon polariton resonators. *Nano Lett.* **2013**, *13*, 3690–3697.

(13) Chen, Y.; Francescato, Y.; Caldwell, J. D.; Giannini, V.; Maß, T. W. W.; Glembocki, O. J.; Bezares, F. J.; Taubner, T.; Kasica, R.; Hong,

DOI: 10.1021/acsomega.7b00726
ACS Omega 2017, 2, 3640–3646

M.; Maier, S. A. Spectral tuning of localized surface phonon polariton resonators for low-loss mid-IR applications. *ACS Photonics* **2014**, *1*, 718−724.
(14) Caldwell, J. D.; Vurgaftman, I.; Tischler, J. G.; Glembocki, O. J.; Owrutsky, J. C.; Reinecke, T. L. Atomic-scale photonic hybrids for mid-infrared and terahertz nanophotonics. *Nat. Nanotechnol.* **2016**, *11*, 9−15.
(15) Liu, Y.; Willis, R. F. Plasmon-phonon strongly coupled mode in epitaxial graphene. *Phys. Rev. B: Condens. Matter Mater. Phys.* **2010**, *81*, 081406.
(16) Koch, R. J.; Seyller, T.; Schaefer, J. A. Strong phonon-plasmon coupled modes in the graphene/silicon carbide heterosystem. *Phys. Rev. B: Condens. Matter Mater. Phys.* **2010**, *82*, 201413.
(17) Yan, H.; Low, T.; Zhu, W.; Wu, Y.; Freitag, M.; Li, X.; Guinea, F.; Avouris, P.; Xia, F. Damping pathways of mid-infrared plasmons in graphene nanostructures. *Nat. Photonics* **2013**, *7*, 394−399.
(18) Zhu, X.; Wang, W.; Yan, W.; Larsen, M. B.; Bøggild, P.; Pedersen, T. G.; Xiao, S.; Zi, J.; Mortensen, N. A. Plasmon−phonon coupling in large-area graphene dot and antidot arrays fabricated by nanosphere lithography. *Nano Lett.* **2014**, *14*, 2907−2913.
(19) Dai, S.; et al. Graphene on hexagonal boron nitride as a tunable hyperbolic metamaterial. *Nat. Nanotechnol.* **2015**, *10*, 682−686.
(20) Woessner, A.; Lundeberg, M. B.; Gao, Y.; Principi, A.; Alonso-González, P.; Carrega, M.; Watanabe, K.; Taniguchi, T.; Vignale, G.; Polini, M.; Hone, J.; Hillenbrand, R.; Koppens, F. H. L. Highly confined low-loss plasmons in graphene−boron nitride heterostructures. *Nat. Mater.* **2015**, *14*, 421−425.
(21) Brar, V. W.; Jang, M. S.; Sherrott, M.; Kim, S.; Lopez, J. J.; Kim, L. B.; Choi, M.; Atwater, H. Hybrid surface-phonon-plasmon polariton modes in graphene/monolayer h-BN heterostructures. *Nano Lett.* **2014**, *14*, 3876−3880.
(22) Barcelos, I. D.; Cadore, A. R.; Campos, L. C.; Malachias, A.; Watanabe, K.; Taniguchi, T.; Maia, F. C. B.; Freitas, R.; Deneke, C. Graphene/h-BN plasmon−phonon coupling and plasmon delocalization observed by infrared nano-spectroscopy. *Nanoscale* **2015**, *7*, 11620−11625.
(23) Li, Y.; Yan, H.; Farmer, D. B.; Meng, X.; Zhu, W.; Osgood, R. M.; Heinz, T. F.; Avouris, P. Graphene plasmon enhanced vibrational sensing of surface-adsorbed layers. *Nano Lett.* **2014**, *14*, 1573−1577.
(24) Huck, C.; Vogt, J.; Neuman, T.; Nagao, T.; Hillenbrand, R.; Aizpurua, J.; Pucci, A.; Neubrech, F. Strong coupling between phonon-polaritons and plasmonic nanorods. *Opt. Express* **2016**, *24*, 25528−25539.
(25) Li, X. F.; Yu, S. F. Modeling of Rabi splitting in quantum well microcavities using time-dependent transfer matrix method. *Opt. Express* **2008**, *16*, 19285−19290.
(26) Törmä, P.; Barnes, W. L. Strong coupling between surface plasmon polaritons and emitters: a review. *Rep. Prog. Phys.* **2015**, *78*, 013901.
(27) Kavokin, A. V.; Baumberg, J. J.; Malpuech, G.; Laussy, F. P. *Microcavities*; OUP: Oxford, 2011; Vol. *16*.
(28) Todisco, F.; Esposito, M.; Panaro, S.; De Giorgi, M.; Dominici, L.; Ballarini, D.; Fernández-Domínguez, A. I.; Tasco, V.; Cuscunà, M.; Passaseo, A.; Ciracì, C.; Gigli, G.; Sanvitto, D. Toward Cavity Quantum Electrodynamics with Hybrid Photon Gap-Plasmon States. *ACS Nano* **2016**, *10*, 11360−11368.
(29) Francescato, Y.; Giannini, V.; Yang, J.; Huang, M.; Maier, S. A. Graphene sandwiches as a platform for broadband molecular spectroscopy. *ACS Photonics* **2014**, *1*, 437−443.
(30) Koppens, F. H. L.; Chang, D. E.; de Abajo, F. J. G. Graphene plasmonics: a platform for strong light−matter interactions. *Nano Lett.* **2011**, *11*, 3370−3377.
(31) Francescato, Y. New frequencies and geometries for plasmonics and metamaterials. Ph.D. Thesis, Imperial College London, 2014.
(32) Du, L.; Tang, D.; Yuan, X. Edge-reflection phase directed plasmonic resonances on graphene nano-structures. *Opt. Express* **2014**, *22*, 22689−22698.
(33) Zhao, B.; Zhang, Z. M. Strong plasmonic coupling between graphene ribbon array and metal gratings. *ACS Photonics* **2015**, *2*, 1611−1618.
(34) Rivas, J. G.; Vecchi, G.; Giannini, V. Surface plasmon polariton-mediated enhancement of the emission of dye molecules on metallic gratings. *New J. Phys.* **2008**, *10*, 105007.
(35) Giannini, V.; Zhang, Y.; Forcales, M.; Rivas, J. G. Long-range surface polaritons in ultra-thin films of silicon. *Opt. Express* **2008**, *16*, 19674−19685.
(36) Schlather, A. E.; Large, N.; Urban, A. S.; Nordlander, P.; Halas, N. J. Near-field mediated plexcitonic coupling and giant Rabi splitting in individual metallic dimers. *Nano Lett.* **2013**, *13*, 3281−3286.

DOI: 10.1021/acsomega.7b00726
ACS Omega 2017, 2, 3640−3646